PROCEEDINGS
OF THE
30th ANNUAL SYMPOSIUM ON
FREQUENCY CONTROL

1976

PROCEEDINGS

of the

THIRTIETH ANNUAL FREQUENCY CONTROL SYMPOSIUM

1976

Sponsored By

U.S. ARMY ELECTRONICS COMMAND
Fort Monmouth, N.J.
Major General A. B. Crawford, Jr.
Commanding

ELECTRONICS TECHNOLOGY AND DEVICES LABORATORY
Dr. Hans K. Ziegler
Director

Copies of the Proceedings are available from:

Electronic Industries Association
2001 Eye Street, N.W.
Washington, D.C. 20006

PRICE PER COPY: $8.00

2 - 4 June 1976
Howard Johnson's Motor Lodge
Atlantic City, New Jersey

THIRTIETH ANNUAL FREQUENCY CONTROL SYMPOSIUM

Sponsored By

U.S. ARMY ELECTRONICS COMMAND

ELECTRONICS TECHNOLOGY AND DEVICES LABORATORY

Fort Monmouth, New Jersey

2 – 4 June 1976

Howard Johnson's Motor Lodge

Atlantic City, New Jersey

SYMPOSIUM EXECUTIVE COMMITTEE

Co-Chairman	Mr. Milton Tenzer
Co-Chairman	Dr. Erich Hafner
Executive Assistant	Dr. John Vig
Secretary	Mrs. Lee Hildebrandt

TECHNICAL PROGRAM COMMITTEE

Dr. Erich Hafner-Chairman
U.S. Army Electronics Command

Mr. Edward Alexander
Bell Laboratories

Dr. Art Ballato
U.S. Army Electronics Command

Mr. Andy Chi
NASA—Goddard Space Flight Center

Dr. Lewis Claiborne
Texas Instruments

Dr. Cecil Costain
National Research Council

Dr. Dick Damerow
Sandia Laboratories

Mr. Joe Giannotto
U.S. Army Electronics Command

Dr. Don Hammond
Hewlett—Packard

Dr. Helmut Hellwig
National Bureau of Standards

Mr. John Holmbeck
Northern Engineering Laboratories

Mr. Erich Kentley
C.R. Snelgrove

Mr. Art Machlin
U.S. Army Materiel Dev. & Readiness Cmd.

Mr. Pete Maresca
U.S. Army Satellite Comm. Agency

Mr. Dennis Reifel
Motorola

Mr. Lauren Rueger
Johns Hopkins University

Mr. Stan Schodowski
U.S. Army Electronics Command

Mr. John Sherman
General Electric

Dr. Richard Sydnor
Jet Propulsion Laboratory

Dr. Robert Vessot
Smithsonian Astrophysical Laboratory

Mr. Ted Viars
U.S. Army Electronics Command

Dr. John Vig
U.S. Army Electronics Command

Dr. Gernot Winkler
U.S. Naval Observatory

CHAIRMEN FOR TECHNICAL SESSIONS

NONLINEAR STRESS/STRAIN PHENOMENA

Dr. R. N. Thurston, Bell Laboratories

RESONATOR DESIGN AND MEASUREMENT

Mr. Edward J. Alexander, Bell Laboratories

CRYSTAL FILTERS AND MATERIAL PROPERTIES

Dr. Hans Jaffe

THEORY AND DESIGN OF RESONATORS (INCLUDING QUARTZ WATCH CRYSTALS)

Dr. Virgil E. Botton, TYCO Crystal Products, Inc.

RESONATOR PROCESSING TECHNIQUES

Mr. John H. Sherman, Jr. General Electric

FREQUENCY GENERATION AND MEASUREMENT

Mr. Marvin E. Frerking, Collins Radio Co.

SURFACE WAVE DEVICES

Dr. Lewis Claiborne, Texas Instruments

FREQUENCY AND TIME - SYNCHRONIZATION, DISTRIBUTION AND APPLICATION

Col. William G. Huston, US Air Force

ATOMIC AND MOLECULAR FREQUENCY STANDARDS

Prof. N. F. Ramsey, Harvard University

DISCUSSION PANEL ON REMOTE SYNCHRONIZATION TECHNIQUES

Moderator - L. J. Rueger, The Johns Hopkins University

Panel: Mr. David Allan, National Bureau of Standards
Dr. Carroll Alley, University of Maryland
Dr. Thomas Clark, NASA - Goddard Space Flight Center
LCDR William Jones, US Coast Guard
Col. William G. Huston, US Air Force
Dr. Burton R. Saltzberg, Bell Laboratories
Dr. A. J. Van Dierendonck, General Dynamics
Dr. G. M. R. Winkler, US Naval Observatory

TABLE OF CONTENTS

EFFECTS OF ACCELERATION ON THE RESONNANCE FREQUENCIES OF CRYSTAL PLATES

P. C. Y. Lee and Kuang-Ming Wu
Department of Civil Engineering
Princeton University
Princeton, New Jersey

Summary

The changes in the thickness-shear resonnance frequencies of circular crystal plates subjected to steady in-plane acceleration with arbitrary direction are studied.

A closed form solution for a circular plate under acceleration with three or more points of mounting is obtained. From this solution, initial stress and strain fields are computed at each and every point of the plate as a function of plate orientation, direction of acceleration, and positions of supports. These fields are then taken into account in the coupled equations of the incremental thickness-shear and flexural vibrations through the second- and third-order elastic stiffness coefficients of the crystal.

Due to the space-dependence or non-uniformity of the initial fields and the smallness of the frequency changes, ($\Delta f/f_o$ in the order of 10^{-9}) a perturbation method is used to calculate the changes in the thickness-shear resonnances. The predicted frequency changes are computed as functions of the acceleration direction and of the positions of the supports for AT cut of quartz. These are then compared with experimental values of A. W. Warner and W. L. Smith.

Introduction

This is the third in a series of studies of the frequency-sensitivity of crystal resonator plates to external forces. In the first paper of the series,[1] a system of six two-dimensional equations, accommodating the coupling of the flexure, extension, face-shear, thickness-shear and thickness-twist modes, was derived for vibrations or waves of small-amplitude superimposed on finite, elastic deformations due to static, initial stresses. In these equations, the nonlinear terms associated to the third-order elastic stiffnesses in stress-strain relations were included. Then the frequency changes of the fundamental thickness-shear modes of circular rotated Y-cuts of quarts, subjected to a pair of diametrical forces, were studied and compared with various existing experimental data.[2-5] In the second paper,[6] nonlinear effects of initial bending on the vibrations of circular quartz plates were investigated. The plate was flexed as a cantilever near the edge and stressed by a transverse, concentrated force applied at a point diametrically opposite the support. In obtaining the initial fields caused by bending, strain components were assumed to be small, but large gradients of plate deflection and large rotations of the plate element are permissible by retaining their quadratic terms in strain-displacement relations. Predicted values were compared with the measured ones by Mingins, Barcus, and Perry.[3] In both cases, explicit formulas for predicting frequency changes were obtained in terms zero- and first-order strains through the second- and third-order elastic stiffness coefficients.

In the present paper, the equations of motion for the coupled thickness-shear and flexural vibrations derived in Ref. 1 are employed in the studies of the acceleration effects on the changes in thickness-shear resonances. Experimental investigations on acceleration effects have been done by A. W. Warner,[7] W. L. Smith,[8] and by M. Valdois, J. J. Gagnepain and J. Besson.[9]

Circular Plate Under In-Plane Acceleration

A circular plate of radius R is referred to the rectangular coordinates X, Y, Z with XZ plane as the middle plane of the plate. The plate is supported by a number of metal ribbons attached to the edge of the plate. Their locations are denoted by angles α_i, $i = 1,2,\ldots n$ for n supports (See Fig. 1). The plate is subjected to a steady in-plane body force G with its orientation denoted by angle ϕ with respect to X-axis. This problem is analyzed in two stages. In this section, initial fields due to the acceleration are determined. Then the small oscillations superimposed on the initial fields are studied in the next section.

Equilibrium of Forces and Moments

Let N_i and T_i denote the normal and tangential components, respectively, of the force from the support at α_i to the plate (See Fig. 1). For the equilibrium of the plate under the body force G (force per unit volume), we require

$$\begin{aligned}
&\Sigma F_x = 0 \\
&\quad G\ 2b\ \pi\ R^2 \cos\phi + \sum_{i=1}^{n} N_i \cos\alpha_i - \sum_{i=1}^{n} T_i \sin\alpha_i = 0 \\
&\Sigma F_z = 0 \\
&\quad G\ 2b\ \pi\ R^2 \sin\phi + \sum_{i=1}^{n} N_i \sin\alpha_i + \sum_{i=1}^{n} T_i \cos\alpha_i = 0 \\
&\Sigma M_y = 0 \\
&\qquad \sum_{i=1}^{n} T_i = 0
\end{aligned} \tag{1}$$

Force-Displacement Relations

Let u_i and w_i denote the normal and tangential components, respectively, of the displacement of the support at α_i. Assume that the response of each metal ribbon can be represented by a cantilever beam subjected to end forces N_i and T_i. Then for a metal ribbon of length ℓ, and rectangular cross-section area $h_1 \times h_2$, the force-displacement relations are,[10]

$$N_i = -\ K\ I_1\ u_i\ , \quad T_i = -\ K\ I_2\ w_i \tag{2}$$

where $K = 3E/\ell^3$, $I_1 = h_2 h_1^3/12$, and $I_2 = h_1 h_2^3/12$. We note that

$$\gamma \equiv I_1/I_2 = h_1^2/h_2^2 << 1..$$

Compatibility of Displacements of Supports

Let u and w be the rigid body displacements in X and Z directions, respectively, and α the rigid body rotation about Y axis of the plate. Assume that relative displacements between any pair of material particles within the plate caused by the initial body force are small as compared with the rigid body translations u and w. Then the compatibility relations

among the displacements of the supports are

$$u_i = u \cos \alpha_i + w \sin \alpha_i$$
$$w_i = - u \sin \alpha_i + w \cos \alpha_i + R \alpha \tag{3}$$

We have thus obtained from eqs. (1) - (3) a system of (4 x n + 3) equations with u_i, w_i, N_i, T_i, u, w, and α as the (4 x n + 3) unknowns. It can be reduced to a system of three equations in terms of u, w, and α by substituting (3) into (2) and, in turn, into (1) as follows.

$$\begin{bmatrix} -\gamma \Sigma c_i^2 - \Sigma s_i^2 & -(1-\gamma) \Sigma s_i c_i & \Sigma s_i \\ (1-\gamma) \Sigma s_i c_i & -\gamma \Sigma s_i^2 - \Sigma c_i^2 & -\Sigma c_i \\ -\Sigma c_i & \Sigma s_i & n \end{bmatrix} \begin{bmatrix} u \\ w \\ R\alpha \end{bmatrix} = \begin{bmatrix} -\bar{G} \cos \\ -\bar{G} \sin \\ 0 \end{bmatrix} \tag{4}$$

where

$$\bar{G} = \frac{2b \pi R^2}{K I_2} G, \quad s_i = \sin \alpha_i, \quad c_i = \cos \alpha_i.$$

Once u, w, and α are obtained from (4), we can compute support displacements from (3) and support forces from (2).

Initial Stress Field

The exact solution for an isotropic circular plate which is subjected to body force G and boundary forces N_i and T_i may be obtained from Michell's solutions[11] in plane-stress theory of elasticity. The rectangular components of stress at a point P(x,z) are given by

$$\sigma_x = \sum_{i=1}^{n} (\sigma_{x_i} - \frac{N_i}{4\pi bR}) - \frac{1}{2} G_x x + \frac{1}{2} G_z z$$
$$\sigma_z = \sum_{i=1}^{n} (\sigma_{z_i} - \frac{N_i}{4\pi bR}) + \frac{1}{2} G_x x - \frac{1}{2} G_z z \tag{5}$$
$$\tau_{xz} = \sum_{i=1}^{n} T_{xz_i} - \frac{1}{2} G_x z - \frac{1}{2} G_z x$$

where $G_x = \cos \phi$, $G_z = G \sin \phi$.

σ_{r_i} is the normal stress at point P(x,z) due to forces N_i and T_i applied at point $A_i(x_i,z_i)$. It is a normal stress acting in the direction $\overrightarrow{PA_i}$ or along r_i (See Fig. 2) and is given by

$$\sigma_{r_i} = \frac{1}{\pi b r_i} (N_i \cos \theta_i + T_i \sin \theta_i) \tag{6}$$

or in rectangular components

$$\sigma_{x_i} = \sigma_{r_i} \cos^2 \beta_i$$
$$\sigma_{z_i} = \sigma_{r_i} \sin^2 \beta_i \tag{6}'$$
$$\tau_{xz_i} = \sigma_{r_i} \sin \beta_i \cos \beta_i.$$

Once the locations of points A_i and P, or α_i, x_i, z_i, x, and z, are given, the other quantities in the above equations may be obtained through geometrical considerations as follows.

$$\cos \theta_i = \frac{1}{r_i R} (R^2 - z_i z - x_i x)$$
$$\sin \theta_i = \frac{1}{r_i R} (z_i x - x_i z)$$
$$r_i^2 = (x - x_i)^2 + (z - z_i)^2 \tag{7}$$
$$\beta_i = (\alpha_i + \theta_i) \pm 2 m \pi$$

where m is an integer so chosen that $0 \leq \beta_i \leq \pi$.

Initial Strain Field

Due to the symmetry of the applied forces and the plate itself with respect to XZ plane, we take $U_1^{(0)}$, $U_3^{(0)}$ and $U_2^{(1)}$ as the non-zero initial displacement components. Then by linearizing the initial strain-displacement relations, eqs. (53) of Ref. 1, we have

$$E_1^{(0)} = U_{1,1}^{(0)}, \quad E_3^{(0)} = U_{3,3}^{(0)}$$
$$E_2^{(0)} = U_2^{(1)}, \quad 2E_5^{(0)} = U_{1,3}^{(0)} = U_{3,1}^{(0)} \tag{8}$$

For the last relation of (8), it is assumed that in-plane rotation associated with initial deformation is negligible,

i.e. $(U_{1,3}^{(0)} + U_{3,1}^{(0)})/2 = 0.$

The above strain components may be computed from the initial stress-strain relations, eqs. (49) of Ref. 1,

$$T_p^{(0)} = 2b \, C_{pq} \, E_q^{(0)} \tag{9}$$

where $T_p^{(0)}$ are related to components of initial stress obtained from (5) by following relations.

$$T_1^{(0)} = 2b\sigma_x, \quad T_3^{(0)} = 2b\sigma_z$$
$$T_{13}^{(0)} = 2b \, \tau_{xz}. \tag{10}$$

The initial stress field is calculated from (5) for a circular plate with four supports. Two of the supports are along the x_1 axis and the other two along the x_3 axis. The plate is subjected to a body force G = 15 g in the $-x_1$ axis direction. The distribution of stress components along diameters oriented in x_1 direction, 45° from x_1, x_3 direction, and 9° from x_3 are shown in Figs. 3-6, respectively. Stresses due to forces which are statically equivalent to those calculated from (2), but uniformaly distributed over the supported area are also calculated and are shown in dashed lines in Figs. 5-6. The comparison shows that the differences are not significant in the electroded central area, but they are more pronounced near the edge of the plate.

Thickness-Shear and Flexural Incremental Vibrations

For rotated Y-cuts of quartz vibrating in the vicinity of the thickness-shear frequencies, the predominent component of incremental displacement is $u_1^{(1)}$ which is coupled to $u_2^{(0)}$. The coupled equations of motion of thickness-shear and flexural modes with $U_i^{(0)}$, $E_p^{(0)}$ and $T_p^{(0)}$ of (8) and (9) as unknown functions of x_1 and x_3 are obtained from eqs. (55) of Ref. 1 as follows.

$$\frac{\partial}{\partial x_1}[(1+U_2^{(0)})t_6^{(0)}+U_{2,1}^{(0)}t_1^{(1)}+U_{2,3}^{(1)}t_5^{(1)}+T_1^{(0)}u_{2,1}^{(0)}]$$

$$+\frac{\partial}{\partial x_3}[(1+U_2^{(1)})t_4^{(0)}+U_{2,1}^{(1)}t_5^{(1)}+U_{2,3}^{(1)}t_3^{(1)}$$

$$+T_5^{(0)}u_{2,1}^{(0)}] = 2b\rho\,\ddot{u}_2^{(0)} \qquad (11)$$

$$\frac{\partial}{\partial x_1}[(1+U_{1,1}^{(0)})t_1^{(1)}+U_{1,3}^{(0)}t_5^{(1)}]+\frac{\partial}{\partial x_3}[(1+U_{1,1}^{(0)})t_5^{(1)}$$

$$+U_{1,3}^{(0)}t_3^{(1)}]-[(1+U_{1,1}^{(0)})t_6^{(0)}+U_{1,3}^{(0)}t_4^{(0)}$$

$$+T_2^{(0)}u_1^{(1)}] = \frac{2}{3}\rho\,b^3\,\ddot{u}_1^{(1)}$$

where the incremental stress-strain relations, eqs. (50) of Ref. 1, are

$$t_p^{(0)} = 2b\,(C_{pq}+C_{pqr}E_r^{(0)})\kappa_{(p)}\,\kappa_{(q)}\,\eta_q^{(0)}$$

$$t_p^{(1)} = \frac{2}{3}b^3\,(C_{pq}+C_{pqr}E_r^{(0)})\,\eta_q^{(1)} \qquad (12)$$

and the incremental strain-displacement relations, eqs. (53) of Ref. 1, are

$$\eta_4^{(0)} = U_{1,3}^{(0)}\,u_1^{(1)}$$

$$\eta_6^{(0)} = (1+U_2^{(1)})\,u_{2,1}^{(0)} + (1+U_{1,1}^{(0)})\,u_1^{(1)}$$

$$\eta_1^{(1)} = U_{2,1}^{(1)}\,u_{2,1}^{(0)} + (1+U_{1,1}^{(0)})\,u_{1,1}^{(1)} \qquad (13)$$

$$\eta_5^{(1)} = U_{2,3}^{(1)}\,u_{2,1}^{(0)} + U_{1,3}^{(0)}\,u_{1,1}^{(1)}$$

The displacement equations of motion of $u_1^{(1)}(x_1,t)$ and $u_2^{(0)}(x_1,t)$ are obtained by substituting (13) into (12) then into (11). The resulting equations in terms of dimensionless variables

$$\phi = u_1^{(1)} \quad , \quad u = u_2^{(0)}/b \qquad (14)$$

are

$$\bar{T}_1\partial_{11}\phi + \bar{T}_2\partial_1\phi + \bar{T}_3\phi + \bar{T}_4\partial_{11}u + \bar{T}_5\partial_1 u = -\Omega^2\phi$$

$$\bar{F}_1\partial_{11}\phi + \bar{F}_2\partial_1\phi + \bar{F}_3\phi + \bar{F}_4\partial_{11}u + \bar{F}_5\partial_1 u = -3\Omega^2 u \qquad (15)$$

where $\bar{T}_i$ and $\bar{F}_i$ are functions of initial fields and material constants C_{pq} and C_{pqr}. The space dependence of these functions through the initial fields makes the exact solutions of (15) very difficult to obtain. A careful examination of these functions reveal that each function can be separated into two parts as

$$\bar{T}_i = T_i + t_i$$
$$\bar{F}_i = F_i + f_i \qquad (16)$$

where T_i, F_i are associated vibrational motion without initial stresses and dependent on material properties only, while t_i, f_i are contributed by initial fields and are space dependent. Expressions of these functions are given as follows.

$$\bar{T}_1 = \frac{b^2}{3\kappa_1^2 C_{66}}[(1+2U_{1,1}^{(0)})\,C_{11}^{(0)}+2U_{1,3}^{(0)}C_{15}^{(0)}]$$

$$\bar{T}_2 = \frac{b^2}{3\kappa_1^2 C_{66}}[2U_{1,11}^{(0)}\,C_{11}^{(0)}+U_{1,33}^{(0)}(C_{13}^{(0)}+C_{55}^{(0)})$$

$$+4\,U_{1,13}^{(0)}C_{15}^{(0)}+(1+2U_{1,1}^{(0)})\,C_{11r}\,E_{r,1}^{(0)}$$

$$+4\,U_{1,3}^{(0)}C_{15r}E_{r,1}^{(0)}+U_{1,3}^{(0)}(C_{13r}+C_{55r})E_{r,3}^{(0)}]$$

$$\bar{T}_3 = \frac{1}{C_{66}}[(1+2U_{1,1}^{(0)})C_{66}^{(0)}+2U_{1,3}^{(0)}C_{64}^{(0)}] \qquad (17)$$

$$\bar{T}_4 = \frac{b^3}{3\kappa_1^2 C_{66}}(U_{2,1}^{(1)}C_{11}^{(0)}+U_{2,3}^{(1)}\,C_{15}^{(0)})$$

$$\bar{T}_5 = \frac{b^3}{3\kappa_1^2 C_{66}}[U_{2,11}^{(1)}C_{11}^{(0)}+2U_{2,13}^{(1)}C_{15}^{(0)}+U_{2,33}^{(0)}C_{55}^{(0)}$$

$$+U_{2,1}^{(1)}\,(C_{11r}E_{r,1}^{(0)}+C_{15r}E_{r,3}^{(0)})$$

$$+U_{2,3}^{(1)}\,(C_{51r}E_{r,1}^{(0)}+C_{55r}E_{r,3}^{(0)})]$$

$$-\frac{b}{C_{66}}[(1+U_2^{(1)}+U_{1,1}^{(0)})\,C_{66}^{(0)}+U_{1,3}^{(0)}\,C_{64}^{(0)}]$$

$$\bar{F}_1 = \frac{b^3}{3\kappa_1^2 C_{66}}(U_{2,1}^{(1)}\,C_{11}^{(0)}+U_{2,3}^{(1)}\,C_{15}^{(0)})$$

$$\bar{F}_2 = \frac{b^3}{3\kappa_1^2 C_{66}}[U_{2,11}^{(1)}C_{11}^{(0)}+2U_{2,13}^{(1)}C_{15}^{(0)}+U_{2,33}^{(1)}\,C_{13}^{(0)}$$

$$+U_{2,1}^{(1)}\,(C_{11r}E_{r,1}^{(0)}+C_{15r}E_{r,3}^{(0)})$$

$$+U_{2,3}^{(1)}\,(C_{15r}E_{r,1}^{(0)}+C_{13r}E_{r,3}^{(0)})]$$

$$+\frac{b}{C_{66}}[(1+U_2^{(1)}+U_{1,1}^{(0)})\,C_{66}^{(0)}+U_{1,3}^{(0)}\,C_{64}^{(0)}] \qquad (18)$$

$$\bar{F}_3 = \frac{b}{C_{66}}[(U_{2,1}^{(1)}+U_{1,11}^{(0)})\,C_{66}^{(0)}+(U_{2,3}^{(1)}+2U_{1,13}^{(0)})C_{64}^{(0)}$$

$$+U_{1,33}^{(0)}\,C_{44}^{(0)}+U_{1,3}^{(0)}\,C_{64r}E_{r,1}^{(0)}+U_2^{(1)}C_{64r}E_{r,3}^{(0)}$$

$$+(1+U_2^{(1)}+U_{1,1}^{(0)})\,C_{66r}\,E_{r,1}^{(0)}]$$

$$\bar{F}_4 = \frac{b^2}{2\kappa_1^2 C_{66}}[3\kappa_1^2\,(1+2U_2^{(1)})\,C_{66}^{(0)}+3\,T_1^{(0)}/2b]$$

$$\bar{F}_5 = \frac{b}{2\kappa_1^2 C_{66}}(T_{1,1}^{(0)}+T_{5,3}^{(0)})+\frac{b^2}{C_{66}}[2U_{2,1}^{(1)}C_{66}^{(0)}+2U_{2,3}^{(1)}C_{64}^{(0)}$$

$$+(1+2U_2^{(1)})\,(C_{66r}\,E_{r,1}^{(0)}+C_{64r}\,E_{r,3}^{(0)})]$$

where

$$C_{pq}^{(0)} = C_{pq}+C_{pqr}\,E_r^{(0)} \qquad (19)$$

By setting initial fields to zero in (17) and (18), we have

$$T_1 = \frac{b^2 C_{11}}{3\kappa_1^2 C_{66}}, \quad T_3 = -1, \quad T_5 = -b,$$
$$F_2 = b, \quad F_4 = b^2, \tag{20}$$

and $T_2 = T_4 = F_1 = F_3 = F_5 = 0$. It can be seen that (15) reduce to the coupled equations of thickness-shear and flexural vibrations when there are no initial stresses.[12] For free vibration problems, (15) may be written in the following matrix form.

$$Lv = \lambda v \tag{21}$$

where L is the linear differential operator and is separated into two parts as the following.

$$L = L_o + Q \tag{22}$$

where

$$L_o = \begin{bmatrix} T_1\partial_{11}+T_3 & T_5\partial_1 \\ \frac{1}{3}F_2\partial_1 & \frac{1}{3}F_4\partial_{11} \end{bmatrix} \tag{23}$$

$$Q_o = \begin{bmatrix} t_1\partial_{11}+t_2\partial_1+t_3 & t_4\partial_{11}+t_5\partial_1 \\ \frac{1}{3}(f_1\partial_{11}+f_2\partial_1+f_3) & \frac{1}{3}(f_4\partial_{11}+f_5\partial_1) \end{bmatrix}$$

In (21), v is the displacement in vector form and is related to the dimensionless frequency Ω as follows.

$$v = \begin{bmatrix} \phi \\ u \end{bmatrix}$$
$$\lambda = -\Omega^2 = -(\omega/\omega_1)^2 \tag{24}$$

where $\omega_1 = [3\kappa_1^2 C_{66}/\rho b^2]^{1/2}$ is the lowest thickness-shear cut-off frequency of an infinite plate without initial stresses. We note L_o is the part of the operator associated to motions without initial stresses while Q is the part of the operator which includes all the effects of initial fields. Since the values of t_i and f_i are several orders of magnitude smaller than those of T_i and F_i, respectively, it is appropriate to employ the perturbation method to obtain the frequency changes due to acceleration.

Let

$$\lambda = \lambda_o + \lambda^{(1)}$$
$$v = v_o + v^{(1)} \tag{25}$$

where v_o and λ_o satisfy

$$L_o v_o = \lambda_o v_o \tag{26}$$

(26) are the equations of motion of the thickness-shear and flexural vibrations without initial stresses. Their solution form and dispersion relation may be obtained from eqs. (20), (22), and (24) of Ref. 12. We further impose traction-free boundary conditions $t_{21}^{(0)} = t_{11}^{(1)} = 0$ (from eqs. (61) of Ref. 1), at $x_1 = \pm R$,

$$\partial_1 u + \phi = 0, \quad \partial_1 \phi = 0 \tag{27}$$

and normalization

$$\int_A v_o \cdot v_o \, dA = 1 \tag{28}$$

The changes in the resonance frequencies of the fundamental thickness-shear modes are

$$\frac{\Delta f}{f_o} = \frac{\Omega-\Omega_o}{\Omega_o} = \frac{1}{2}\frac{\int_A v_o \cdot Q \cdot v_o \, dA}{\lambda_o} = F(\theta,\phi,\alpha_i,R/b) \tag{29}$$

We see that frequency change is a function of plate orientation θ, azimuth angle of body force φ, locations of the supports α_i, and the ratio of the radius to thickness of the plate R/b.

Calculations for frequency changes are made for circular AT-cuts of quartz plates with diameter 2R = 15mm, thickness 2b = 1.69 mm. The plate is subjected to an acceleration with G = 15 g = 14700 cm/sec^2 and supported by four nickel ribbons of length ℓ = 6.35 mm and rectangular cross-section (h_1 = 0.076 mm and h_2 = 1.270 mm). The Young's modulus for Nickel is E = 4.82 x 10^9 dyne/cm^2. The predicted frequency changes $\Delta f/f_o$ as a function of azimuth angle φ for three different support configurations are made, using Bechmann's[13] values of the second-order elastic coefficients and those of Thurston, Miskimin, and Andreath[14] for the third-order coefficients. These predicted results are shown in Figs. 7-9 and compared with measured values of Warner[7] and Smith.[8] It can be seen in Figs. 7 and 8 that the agreements of $\Delta f/f_o$ between predicted and measured values are reasonable both in magnitude and variation. In Fig. 9, the measured values are quite different from the calculated values (solid lines) and also different in general character from the measured values for the two plates which have slightly different mounting configurations as shown in Figs. 7 and 8. It appears possible that, in presenting experimental values of $\Delta f/f_o$ for various orientation of accelerations, $-x_3$ axis instead of $+x_3$ axis of the plate was used as the reference. If this is the case, then all the data should be shifted by 180° in abscissa. The calculated values after shifting by 180° are plotted in dotted lines in Fig. 9 for comparison. It is seen that agreement becomes close. When looking at the results, we should keep in mind simplifications have been made in order to obtain the mathematical solutions. The plate is assumed to be uniform in thickness and vibrating at frequencies of the fundamental thickness-shear modes. The actual plates used in experiments are double-convex and excited at frequencies of the fifth overtone of the thickness-shear modes.

Once the accuracy of the analytical solutions are established, the acceleration sensitivity of resonance frequencies can be computed systematically as functions of various effecting factors, i.e. the orientation φ and magnitude G of acceleration, geometry of the resonator plate R/b, positions of the supports α_i, orientation of the plate θ, and the linear and nonlinear material coefficients.

References

1. P. C. Y. Lee, Y. S. Wang, and X. Markenscoff, J. Acoust. Soc. Am. 57, 95-105 (1975). Also Proc.

27th Annu. Freq. Control Symp. 1-6 (1973).

2. A. D. Ballato, Proc. 14th Annu. Freq. Control Symp. 89-114, (1960).

3. A. D. Ballato and R. Bechmann, IRE 48, 261-262 (1960).

4. C. R. Mingins, L. C. Barcus, and R. W. Perry, Repts. 1-20, Lowell Tech. Inst. Found. (1961-66).

5. J. M. Ratajski, IBM J. Res. Dev. 12, 92-99 (1968).

6. P. C. Y. Lee, Y. S. Wang, and X. Markenscoff, J. Acoust. Soc. Am. 59, 90-96 (1970). Also Proc. 28th Annu. Freq. Control Symp. 14-18 (1974).

7. A. W. Warner, Interim Reps. 10-11, Bell Telephone Lab. (1959).

8. W. L. Smith, Interim Reps. 12-13 and Final Rep., Bell Tel. Lab. (1960).

9. M. Valdois, J. J. Gapnepain, and J. Besson, Proc. 28th Annu. Freq. Control. Symp. 19-32 (1974).

10. S. Timoshenko Strength of Materials, Part I, Van Nostrand Company, Inc., N.Y.C. p. 147, (1951).

11. J. H. Michell, Proc. London Math. Soc., 32, 35-61, (1900).

12. R. D. Mindlin and P. C. Y. Lee, Int. J. Solids Structures, 2, 125-139 (1966).

13. R. Bechmann, Phys. Rev. 100, 1060-1061 (1958).

14. R. N. Thurston, H. J. McSkimin, and P. Andreatch, Jr., J. Appl. Phys. 37, 267-275 (1966).

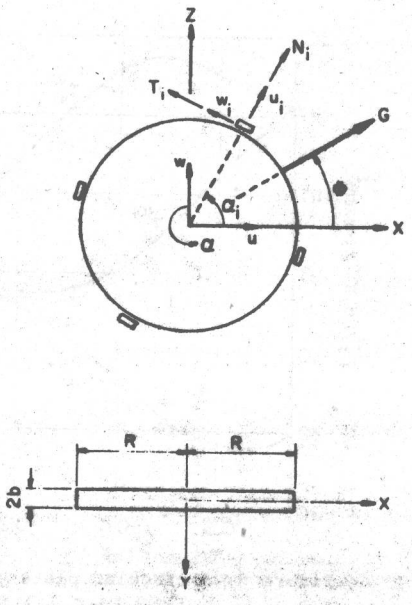

Figure 1 A circular plate under body force G.

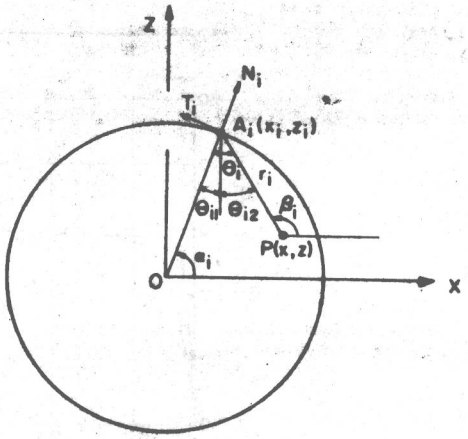

Figure 2 Geometrical relations among α_i, β_i, θ_i, and r_i.

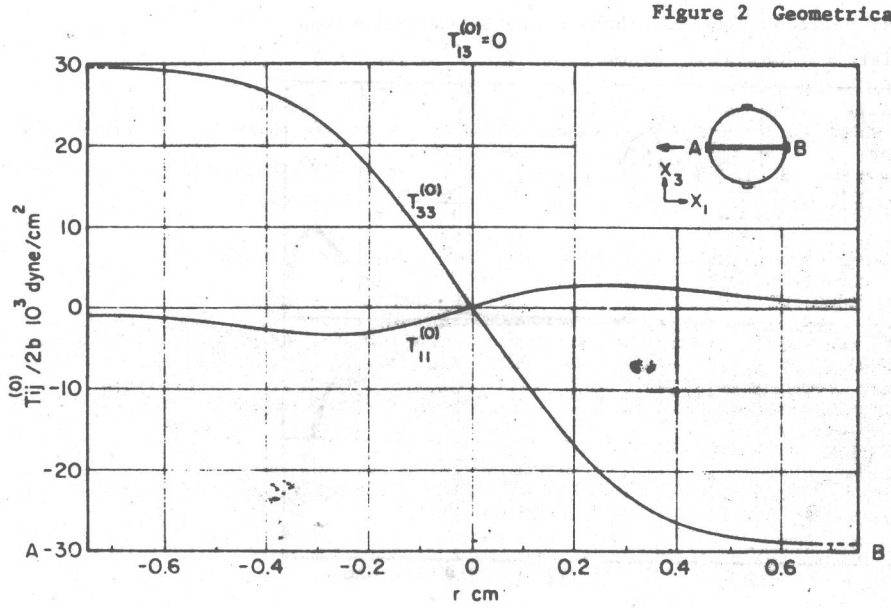

Figure 3 A circular plate subject to a body force in $-x_1$ direction. Stress distributions along diameter $\overline{AB}$ (in x_1 direction).

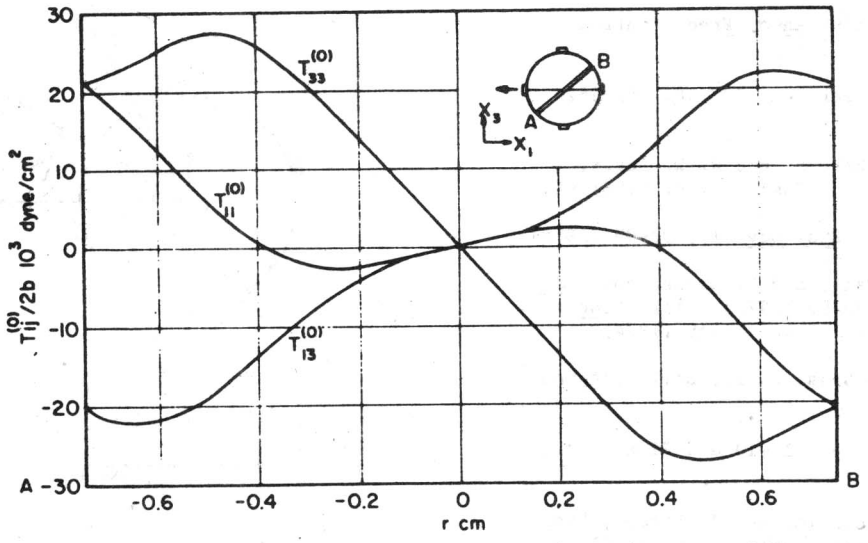

Figure 4 A circular plate subject to a body force in $-x_1$ direction. Stress distributions along diameter $\overline{AB}$ (45° from x_1 axis).

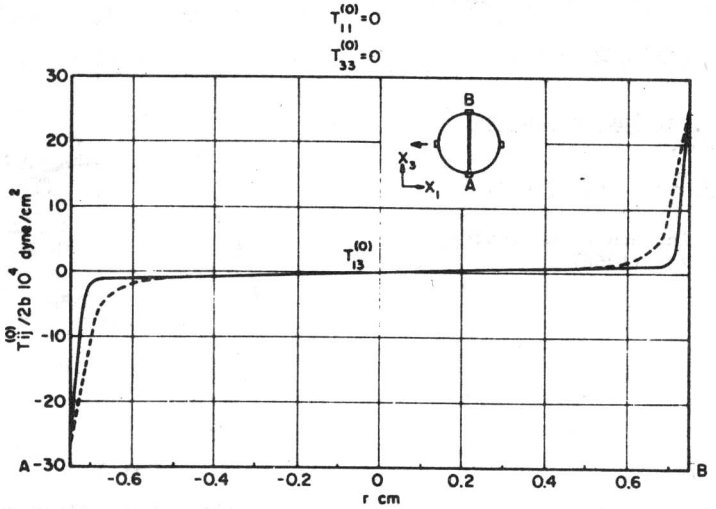

Figure 5 A circular plate subject to a body force in $-x_1$ direction. Stress distributions along diameter $\overline{AB}$ (in x_3 direction).

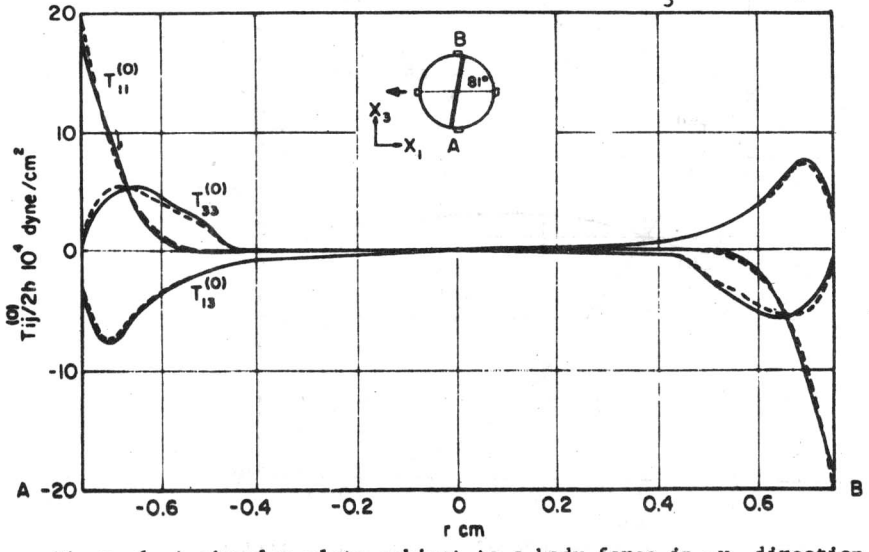

Figure 6 A circular plate subject to a body force in $-x_1$ direction. Stress distributions along diameter $\overline{AB}$ (81° from x_1 axis).

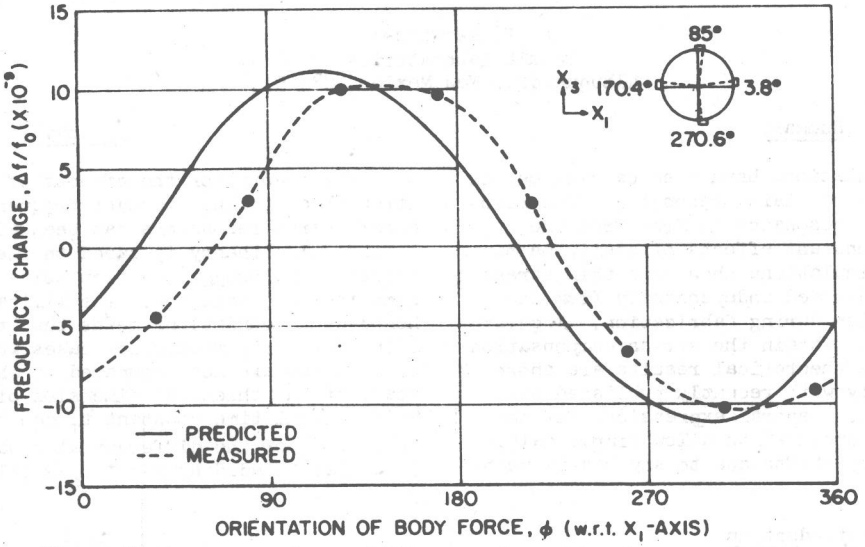

Figure 7 Frequency change $\Delta f/f_o$ as a function of azimuth angle ϕ of body force, for AT-cut plate.

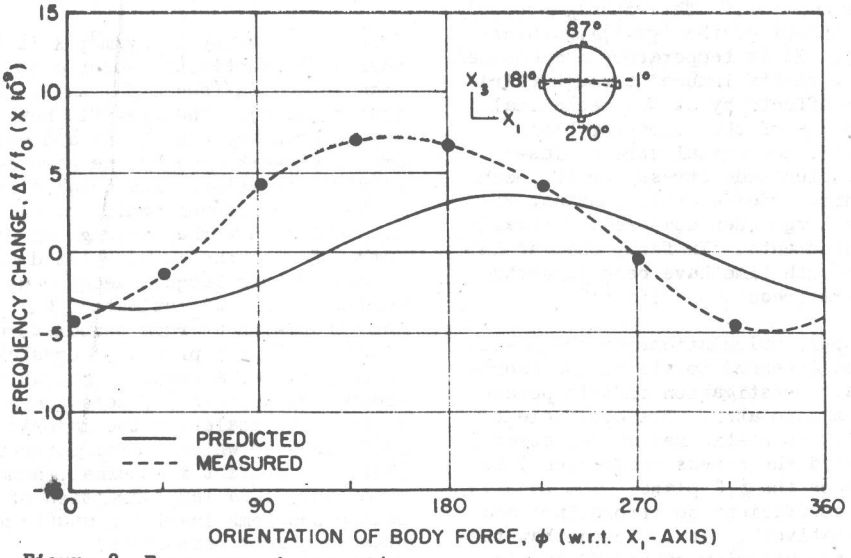

Figure 8 Frequency change $\Delta f/f_o$ as a function of azimuth angle ϕ of body force, for AT-cut plate.

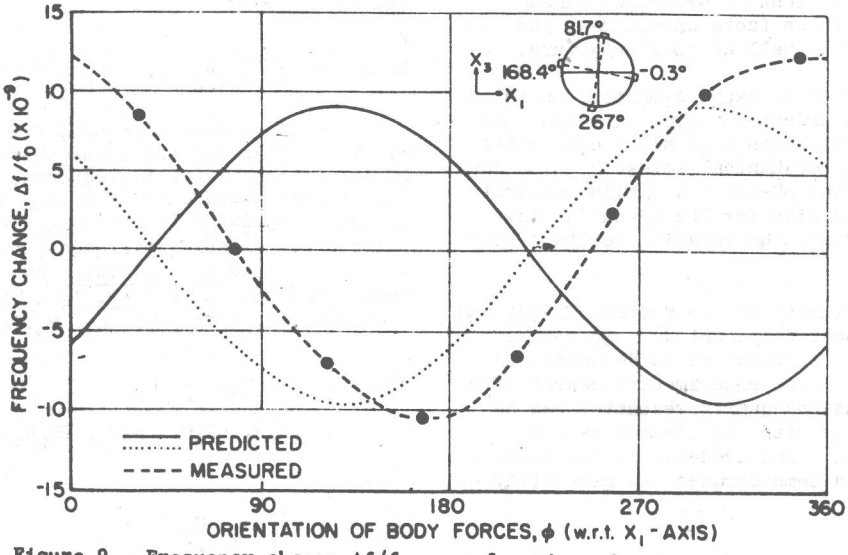

Figure 9 Frequency change $\Delta f/f_o$ as a function of azimuth angle ϕ of body force, for AT-cut plate.

CALCULATIONS ON THE STRESS COMPENSATED (SC-CUT) QUARTZ RESONATOR *

E. P. EerNisse
Sandia Laboratories
Albuquerque, New Mexico 87115

Summary

Theoretical calculations have been carried out on the doubly-rotated SC-cut quartz resonator. The resonant frequency of this resonator is free from the third-order elastic constant effects of static mechanical stress bias. Calculations show that this stress compensation can be adjusted independently from the temperature compensation during fabrication. Angular tolerances necessary to attain the stress compensation are investigated. The theoretical results are shown to agree quantitatively with recently published thermal shock measurements. General expressions for the SC-cut and AT-cut are provided to allow simple calculation of the frequency shifts due to any static mechanical stress bias.

Introduction

The SC-cut was introduced at the 29th Annual Symposium on Frequency Control.[1] This doubly-rotated, quartz resonator is a member of the $(yxwl)\phi,\theta$ thickness-shear mode family. It is temperature compensated and free from frequency shifts induced through third-order elastic constant effects by static mechanical stress biases in the plane of the resonator blank. The sources of the static mechanical stress biases could be acceleration, electrode stress, or the mechanical mounts. The third-order elastic constant effects are surprisingly large when compared to today's frequency control requirements. In fact, changes in mechanical stress bias with time have been suggested as a source of long-term frequency drift.[1,2]

In the present paper, calculations on the SC-cut are presented which are intended to aid in the fabrication and experimental investigation of this potentially important quartz resonator. The coefficient relating frequency shift to static mechanical stress in the electrodes (called the stress coefficient) is shown as contour plots on the ϕ,θ plane. The sensitivity of this stress coefficient to errors in ϕ and θ are discussed quantitatively. It is found that the stress coefficient in the vicinity of the SC-cut is dependent almost entirely on ϕ alone, while the first-order temperature coefficient is dependent almost entirely on θ alone. These facts should make the SC-cut easier to study as well as to manufacture.

A general, quantitative expression for the third-order elastic constant effect in terms of ϕ and θ is presented for the SC-cut which will allow calculation of the influence of any mechanical stress bias on the resonant frequency of the SC-cut. A similar general expression is presented also for the AT-cut so that future workers can compare the relative merits of the SC-cut vs. the AT-cut.

Finally, the similarity of the present SC-cut and the TS-cut (thermal shock compensated) proposed by Holland[3] is discussed. In fact, it is demonstrated that the results of a recent experimental search[4] for a thermal-shock compensated quartz resonator can be explained quantitatively with the present calculations. This comparison lends credence to the existence of the SC-cut and demonstrates the generality of the present calculations.

Theory

The theory for the effects of static mechanical stress bias on the resonant frequency of thickness-shear quartz resonators has been adequately presented before. The theory is based on the formulation by Thurston and Brugger,[5] which holds for isothermal, homogeneous conditions. The limitation of isothermal, homogeneous conditions means that the present calculations apply rigorously for cases where the time scales of interest are long compared to the thermal time constant of the thickness dimension of resonator plates. This thermal time constant t_τ can be estimated from solutions[6] of the differential equation for heat flow in a slab bounded by $x = \pm \tau_q/2$ (plate thickness = τ_q):

$$t_\tau = \frac{\rho C \tau_q^2}{\pi^2 K} \qquad (1)$$

Here ρ is density in kg/m^3; K is the component of the thermal conductivity tensor along the thickness direction in joules/(sec·m·K); and C is specific heat in joules/(kg K). The specific heat depends on the mechanical boundary conditions and varies according to the amount of work done by the stress-strain fields during thermal expansion. The details for the case of a plate heated nonuniformily along the thickness dimension has been worked through by Holland;[7] a typical number for t_τ can be calculated using his numerical values for the largest decay constant and handbook[8] values for K. We estimate[8] K as 8.0 joules/(sec·m·K) for the AT-cut at room temperature. For a 5 MHz, 5th overtone, AT-cut precision crystal thickness of 0.17 cm, t_τ is 71 msec, a result comparable to the 65 msec estimated by Kusters.[4] These times are short relative to to the time scales of the majority of experimental conditions to which quartz resonators are subjected. Thus, the present isothermal, homogeneous theory is applicable to a large fraction of technically interesting problems involving static mechanical stress bias in quartz resonators.

The theoretical formulation can be summed up in the relation[1,5]

$$\Delta f/f = (2\rho_o W_o^2)^{-1}\left[A_\alpha + 2\rho_o W_o^2 U_\beta s_{\alpha\beta} + B_\beta B_\gamma s_{\delta\alpha} C_{\beta\gamma\delta}\right]\Delta\bar{T}_\alpha \qquad (2)$$

Here, matrix notation is used for tensors (α, β, γ, δ run 1-6), f is the thickness shear resonant frequency, Δf is a change in that frequency, ρ_o is mass density in the unstressed condition, $s_{\alpha\beta}$ is the isothermal elastic compliance tensor, $C_{\beta\gamma\delta}$ is the isothermal third-order elastic-stiffness tensor, $\bar{T}_\alpha$ is the average stress bias in the quartz averaged over the thickness dimension τ_q, and $\Delta\bar{T}_\alpha$ is a change in the average static stress bias. The A_α, B_α, and U_α are defined by

$$[A_1, A_2, A_3, A_4, A_5, A_6] = [N_1N_1,\ N_2N_2,\ N_3N_3,\ 2N_2N_3,\ 2N_1N_3,\ 2N_1N_2] \qquad (3)$$

$$[U_1, U_2, U_3, U_4, U_5, U_6] = \left[U_1^oU_1^o,\ U_2^oU_2^o,\ U_3^oU_3^o,\ U_2^oU_3^o,\ U_1^oU_3^o,\ U_1^oU_2^o\right] \qquad (4)$$

$$[B_1, B_2, B_3, B_4, B_5, B_6] = \left[N_1U_1^o,\ N_2U_2^o,\ N_3U_3^o,\ N_2U_3^o + N_3U_2^o,\ N_1U_3^o + N_3U_1^o,\ N_1U_2^o + N_2U_1^o \right] . \quad (5)$$

Here N_i is the unit vector in the direction of acoustic wave propagation (thickness of plate) and W_o^2 and U_i^o are the slow shear wave eigenvalue and eigenvector of

$$\rho_o W_o^2 U_k^o = N_r N_s c_{jrks} U_j^o \quad , \quad (6)$$

where tensor notation is used (subscripts run 1-3) and c_{jrks} is the isothermal elastic stiffness tensor. Piezoelectric effects on resonant frequency are small in quartz and are ignored here.

The values for $\Delta\bar{T}_\alpha$ are found from the specific static stress bias patterns under consideration and are usually identifiable more easily in the plate axes system. A rotation of $\Delta\bar{T}_\alpha$ to the same axes system as that used for the elastic tensors is necessary before the contractions in Eq. (2) can be carried out.

Theoretical Results

The choice of $\Delta\bar{T}_\alpha$ for Eq. (2) is unlimited and a general study is impractical. A planar isotropic stress bias is representative of many experimental situations and is chosen here for the study of stress effects as a function of ϕ and θ. The case of a planar isotropic $\bar{T}_\alpha$ which is generated by an electrode stress has been treated before.[1] Let $\bar{T}_\alpha$ be the average static mechanical stress bias referenced to the plate axes (x_1 is length, x_2 is thickness, x_3 is width). We represent the effect of the electrode stress by the force per unit width, S, acting across the electrode-quartz interface (S is the integral through the electrode thickness of the electrode stress and is in units of dyn/cm). A change in S, ΔS, causes

$$\Delta\tilde{T}_1 = \Delta\tilde{T}_3 = -\Delta S/\tau_q$$
$$\Delta\tilde{T}_2 = \Delta\tilde{T}_4 = \Delta\tilde{T}_5 = \Delta\tilde{T}_6 = 0 \quad (7)$$

in the quartz. Here τ_q is the plate thickness and the minus sign arises because the static stress bias in the quartz is a reaction to the electrode stress (S positive is tension in the electrode). After rotation of $\Delta\tilde{T}_\alpha$ to the crystal axes to find $\Delta\bar{T}_\alpha$, $\Delta S/\tau_q$ can be factored out of $\Delta\bar{T}_\alpha$ to form

$$\frac{\Delta f}{f} = K \frac{\Delta S}{\tau_q} \quad (8)$$

where

$$K = -(2\rho_o W_o^2)^{-1} [A_\alpha + 2\rho_o W_o^2 U_\beta s_{\alpha\beta} + B_\beta B_\gamma s_{\delta\alpha} C_{\beta\gamma\delta}] (\Delta T_\alpha \tau_q/\Delta S) \quad (9)$$

was called the stress coefficient in earlier works[1,9] and is a function of ϕ and θ only.

Contours of K in the (ϕ,θ) plane are shown in Fig. 1 as calculated with published values[10,11] for the various elastic constants in Eq. (9). Included in Fig. 1 is the loci of the zero first-order temperature coefficient.[12] Let us focus our attention first on the SC-cut which is the intersection of the zero contour of K and the zero first-order temperature coefficient at $\phi = 22.4°$ and $\theta = 34.3°$. The contours of K are almost horizontal there. This means that θ can be adjusted around the SC-cut with little effect on K. Likewise, the loci of the zero first-order temperature coefficient is nearly vertical there. This means that ϕ can be adjusted with little effect on the first-order temperature coefficient. This relative orthogonality of the stress effect and the temperature effect has technological impact for it suggests that one can independently adjust the stress and temperature response of the SC-cut.

The right-hand scale of Fig. 1 has been centered on the SC-cut. This was done to allow for the inevitable differences between theoretical calculations and experimental reality which arise both from inaccuracies in the values for the elastic constants and from contouring effects. Noting the right-hand side of Fig. 1, we see that fabrication with an accuracy of $\pm 1.5°$ on ϕ will reduce the stress coefficient by at least a factor of 10 relative to the AT-cut value of 0.273×10^{-11} cm^2/dyn. An accuracy of $\pm 0.2°$ on ϕ during fabrication will provide a reduction in the stress coefficient of at least 100 relative to the AT-cut.

It must be emphasized here that Eq. (9) and the definition of K are specific to the case of stress changes in the electrodes. As such, Eq. (7) leads to the minus sign in Eq. (9) which allows a direct relation between the frequency shifts (Δf) and changes in electrode stresses (ΔS). Equation (2) is the more general relation and should always be used as the starting point for studying the effects of static mechanical stress biases independent of their origin. For this reason, we present here Eq. (2) as evaluated for the SC-cut to facilitate any further work on the effects of arbitrary, static mechanical stress biases. For the SC-cut, we find ($\phi = 22.4°$, $\theta = 34.3°$ in the calculations)

$$\Delta f/f = (-0.1580\ \Delta\bar{T}_1 - 0.08914\ \Delta\bar{T}_2 + 0.1714\ \Delta\bar{T}_3 + 0.2167\ \Delta\bar{T}_4 + 0.3767\ \Delta\bar{T}_5 + 0.3694\ \Delta\bar{T}_6) \times 10^{-11} \quad (10)$$

For comparison, we find for the AT-cut ($\phi = 0°$, $\theta = 35.25°$)

$$\Delta f/f = (-0.2674\ \Delta\bar{T}_1 - 0.05161\ \Delta\bar{T}_2 + 0.2133\ \Delta\bar{T}_3 + 0.2773\ \Delta\bar{T}_4 + 0.0\ \Delta\bar{T}_5 + 0.0\ \Delta\bar{T}_6) \times 10^{-11} \quad (11)$$

In using Eqs. (10) and (11), remember that $\Delta\bar{T}_\alpha$ is referred to the crystal axes, not the resonator plate axes, and $\Delta\bar{T}_\alpha$ is in dyn/cm^2.

Alternately, most workers will find it easier to work in the resonator plate axes (x_1 = length direction x_2 = thickness direction, x_3 = width direction). See Reference 13 for the axes and $(yxwl)\phi,\theta$ conventions used here. Equations (10) and (11) have been rotated to the resonator plate axes; we find for the SC-cut

$$\Delta f/f = (-0.01786\ \Delta\tilde{T}_1 - 0.07560\ \Delta\tilde{T}_2 + 0.01772\ \Delta\tilde{T}_3 + 0.1969\ \Delta\tilde{T}_4 + 0.09044\ \Delta\tilde{T}_5 + 0.2497\ \Delta\tilde{T}_6) \times 10^{-11} \quad (12)$$

and for the AT-cut

$$\Delta f/f = (-0.2674\ \Delta\tilde{T}_1 + 0.1673\ \Delta\tilde{T}_2 - 0.005634\ \Delta\tilde{T}_3 + 0.1711\ \Delta\tilde{T}_4 + 0.0\ \Delta\tilde{T}_5 + 0.0\ \Delta\tilde{T}_6) \times 10^{-11} . \quad (13)$$

In Eqs. (12) and (13), remember that $\Delta\tilde{T}_\alpha$ is in the plate axes system and is in units of dyn/cm^2. For example, with $\Delta\tilde{T}_1 = \Delta\tilde{T}_3 = -1.0$ in Eq. (7), Eq. (12) leads to the $\Delta f/f$ of 0.273×10^{-11}, the value quoted for K of the AT-cut.